

# EFFECT OF LULC CHANGE ON SURFACE RUNOFF IN URBANIZATION AREA

**Zhongchang SUN**

**Huadong GUO**, Director-general

**Xinwu LI**, Associate Director

**Qingni HUANG**

**Daowei ZHANG**

Laboratory of Digital Earth Science

Center for Earth Observation and Digital Earth

Chinese Academy of Sciences

No. 9 Dengzhuang South Road, Haidian District

Beijing, China 100094

zhongchang26@126.com

## ABSTRACT

In recent decades, urbanization has become a significant urban environmental and ecological concern, especially in most developing countries. In China, rapid urban sprawl has had a profound influence on runoff and results in larger and more frequent incidents of flooding in many urban areas. Therefore, evaluating the impacts of urbanization on runoff is of great important for urban planning policy makers and water/land resource management. The objective of this paper is to present a case study to derive land use/land cover (LULC) maps and further to investigate the long-term effects of LULC change on surface runoff in the fast urbanizing Beijing city. The LULC maps were derived from Landsat TM/ETM+ imagery (acquired in 1986, 1992, 1999, 2006, and 2009 respectively) using support vector machine (SVM) method. A Long-Term Hydrologic Impact Assessment (L-THIA) model was applied to assess the impacts of LULC change on surface runoff. Results indicated that the selected study area experienced rapid urbanization from 1986 to 2009. Urban areas increased from 4.18% in 1986 to 12.78% in 2009 in the whole area. Our results also indicated that the long-term surface runoff increased 25% in the whole area from 1986 to 2009, and the runoff increase was highly correlated with urban expansion ( $R^2 = 0.91$ ). This research can provide a simple method for policy makers to assess potential hydrological impacts of future planning and development activities.

**KEYWORDS:** urbanization, LULC, runoff, L-THIA

## INTRODUCTION

Land use/land cover (LULC) changes have direct impacts on the hydrological cycle and stream quality; furthermore, there are also indirect impacts on climate and the subsequent impact of the altered climate on the waters (Weng, 2001). Therefore, LULC changes have been treated as one of the most important sensitive factors for global environmental change. Urbanization is the major force that is driving LULC changes. Although urbanization due to urban sprawl provides social and economic benefits to the community, the detrimental consequences of the

urbanization to the urban environment are widespread, especially in most emerging countries. Increased impervious surface in the urbanization areas can reduce the time of runoff and increase the peak discharges of stream flow, resulting in large and more frequent incidents of flooding (Weng, 2001; Li and Wang 2009). In addition, because of the pollutants in runoff and sediments, the increase of impervious surfaces also degrades stream quality (Li and Wang, 2009). Therefore, urbanized areas would become more susceptible to flood hazard under conditions of high precipitation intensity (Shi *et al.*, 2007).

In recent decades, with a constantly accelerating increase of urban population, urbanization has become a significant urban environmental and ecological concern, especially in most developing countries. Therefore, it is of great significance to accurately map LULC changes in urbanized areas and to evaluate its impacts on surface runoff and stream quality for urban planning policy makers and water/land resource management. Due to their relatively low cost and suitability for large area mapping, satellite remote sensing images have been widely applied for detecting urban growth and accurately and timely mapping LULC changes over a long period (Yang *et al.*, 2003). Furthermore, RS-based LULC changes mapping also allows for a rapid assessment of its impacts on surface runoff and water quality (Li and Wang, 2009). Recently, numerous researchers have assessed the impact of LULC changes induced by urbanization on surface runoff (Ng and Marsalek, 1989; Brun and Band, 2000; Weng, 2001; Lin *et al.*, 2007; Shi *et al.*, 2007; Li and Wang, 2009). Ng and Marsalek (1989) used HSPF to simulate the effects of urbanization on stream flow for the Waterford River Basin near St. John's, Newfoundland, Canada. Brun and Band (2000) also used HSPF to assess the effects of land use change on urbanizing watershed behavior, and the summary expression for the runoff ratio relationship indicates the existence of a threshold percent impervious cover (~20%), above which the runoff ratio changes more dramatically. Weng (2001) used Soil Conservation Service (SCS) model for estimating the effects of urban growth on surface runoff with the integration of remote sensing and GIS; and the results revealed urbanization lowered potential maximum storage and thus increased runoff coefficient values. Shi *et al.* (2007) also used SCS model to assess the effect of LULC change on surface runoff in Shenzhen region, China; the results showed that urbanization played an important factor intensifying the flood process. Li and Wang (2009) used a Long-Term Hydrologic Impact Assessment (L-THIA) model to evaluate the effect of LULC change on surface runoff in Dardenne Creek watershed, St. Louis, Missouri; and results indicated the runoff increase is highly correlated with urban expansion. Zheng *et al.* (2009) used the Soil and Water Assessment Tool (SWAT) model to evaluate the impacts of LULC change on hydrological processes in fast urbanizing region.

To simulate the land use change impacts on watersheds, many hydrologic and water quality models have been developed and integrated with a Geographic Information System (GIS), such as the United States Department of Agriculture (USDA) Technical Release 55 (TR-55) (USDA, 1986), EPA Storm Water Management Model (SWMM) (Huber *et al.*, 1988), and Soil and Water Assessment Tool (SWAT) (Arnold *et al.*, 1998). Although some of these models can be used to assess the long-term impacts of LULC changes on hydrology and stream quality, they require extensive data inputs and parameters that are usually not available for land-use planners (Li and Wang, 2009). Therefore, there has been a need for a much simpler-to-use model to assess relative hydrological impacts of LULC change at the watershed scale. The L-THIA model was developed and integrated with GIS to estimate direct runoff from very basic input data, such as daily rainfall, land uses, and hydrologic soil group (Harbor, 1994; Lim *et al.*, 2006).

In China, rapid urban sprawl has had a profound influence on runoff and results in larger and more frequent incidents of flooding in many urban areas. Over the past three decades, Beijing, the capital of China, is one of the fastest growing urban areas in China, and has undergone intense urbanization that has seriously impacted the urban

surface runoff. The objective of this paper is to derive LULC classification maps and further to quantitatively assess the effects of LULC change on surface runoff in Beijing city. The LULC maps are derived from Landsat TM/ETM+ imagery (acquired in 1986, 1992, 1999, 2006, and 2009 respectively) using support vector machine (SVM) method. To estimate the effects LULC change on runoff, the L-THIA model is used in this research. The rest of this paper is organized as follows: section 2 describes the study area and the datasets used; section 3 discusses methodology; the results and analysis are presented in section 4; and section 5 presents the conclusions.

## STUDY AREA AND DATASETS

### Study Area

Beijing city, the capital of China, was selected as the study area to evaluate the impacts of urbanization on surface runoff (Fig. 1). It is located within 39.28°N-41.05°N and 115.25°E-117.35°E, covering about 16386.30 km<sup>2</sup>. According to soil horizontal zonality, the main soil types are cinnamon soil, moisture soil and brown soil. With warm temperate zone semi-humid continental monsoon climate, the average annual precipitation was 600 mm, and rainfall in the summer season from June to August made up 75% of the annual total. The selected area contains a number of LULC types, including central business district (CBD), high-density residential, low-density residential, agricultural land, forest, exposed soil, and water bodies. Forest land covers 50% of the land area. Over the past three decades, with economic development, Beijing is one of the fastest growing urban areas in China, and has undergone intense urbanization. Beijing's development pattern is a typical concentric expansion; showing a ring-shaped pattern as you move from the inner city to the outskirts.

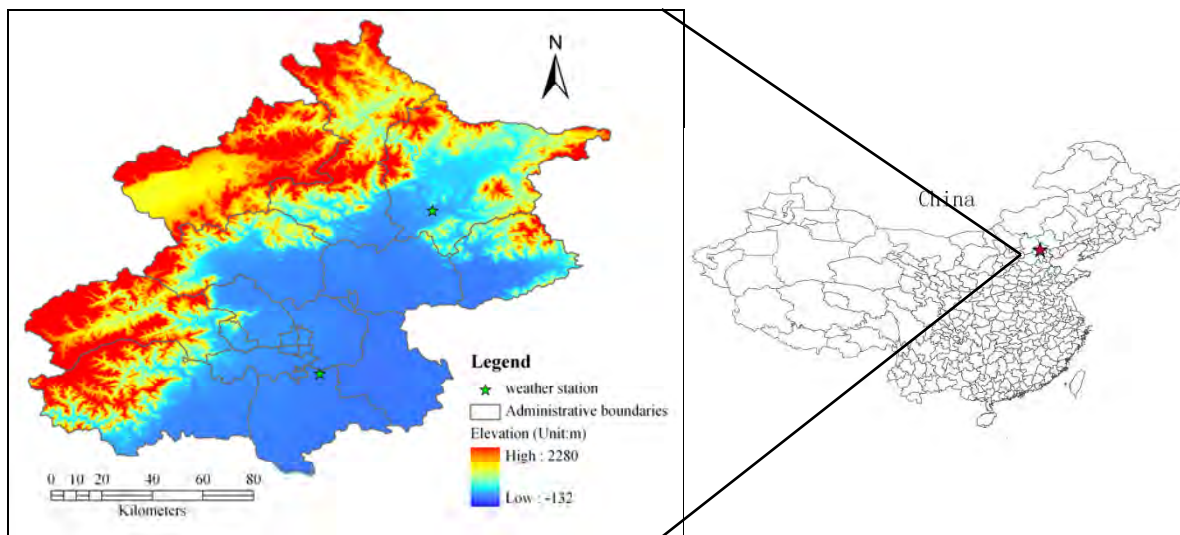


**Figure 1.** Location map of Beijing region. In our study area, there are two weather stations.

### Datasets and Preprocessing

LULC data were derived from Landsat TM/ETM+ imagery (acquired in 1986, 1992, 1999, 2006, and 2009 respectively), with the pixel size of 30 m. The soil type classification map (1:250,000) of study area was obtained from the Soil and Fertilizer Workstations of Beijing. Curve Number (CN) values were used to determine soil hydrological input data. According to four hydrologic soil groups defined by US Soil Conservation Service, the soil

type classification data was reclassified to output the soil hydrological map using ARCVIEW software (Fig. 2). For the purpose of overlaying with same pixel data, the soil hydrological map was rectified to a Universal Transverse Mercator (UTM) coordinate system, with a spatial resolution of 30m. There are two weather stations in the selected area (Fig. 1). Thirty-two years (1978-2009) of precipitation data was obtained from the meteorological department. In addition, the observed daily runoff data was obtained from the gage station; and this data was used for validating the modeled runoff and L-THIA model calibration.

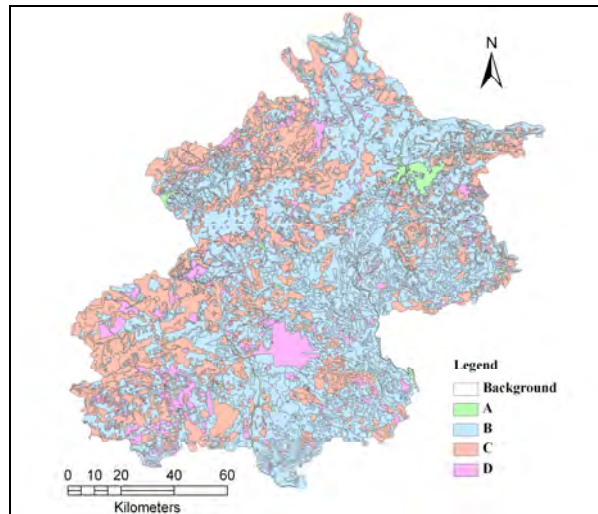


**Figure 2.** Soil hydrology of Beijing. A: high infiltration rate soil; B: moderate infiltration rate soil; C: low infiltration rate soil; D: very low infiltration rate soil.

## METHODOLOGY

In our research, LULC classification maps were derived from long time series Landsat TM/ETM+ imagery. The simpler-to-use L-THIA model integrated with GIS was used to assess the impacts of LULC changes on surface runoff in urbanizing area. Fig. 3 showed the data processing framework of research on hydrological response to LULC changes. In Fig. 3, the figure on the left dashed box was the data processing flowchart of LULC change; while the figure on the right dashed box was the processing flowchart of L-THIA model simulation. In this paper, the robust algorithm, support vector machine (SVM), was selected to perform a supervised classification and further to evaluate the temporal change of LULC in study area. In the following section, only a brief description of SVM algorithm and L-THIA model was given here, respectively.

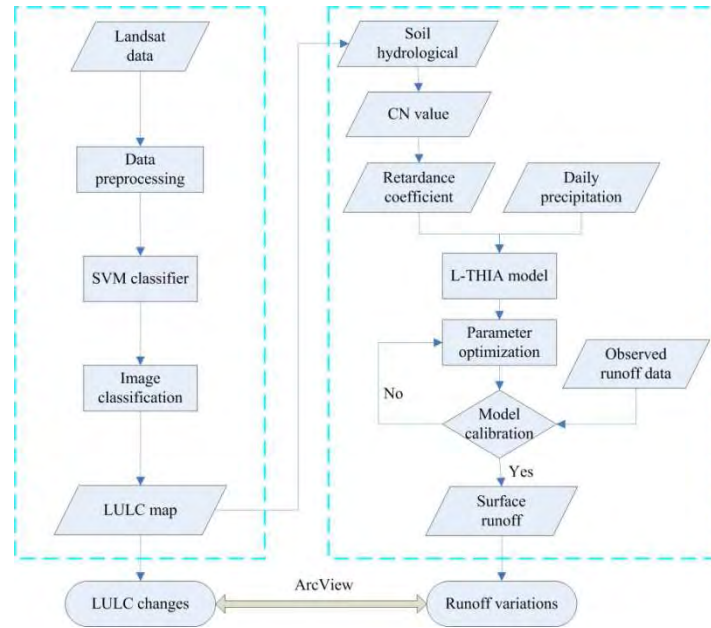


**Figure 3.** The data processing framework of research on hydrological response to LULC changes.

### Support Vector Machine (SVM)

The concept of SVM originated from a nonparametric machine learning methodology based on Vapnik's (1995) Structural Risk Minimization (SRM) principle. The basic idea of SVM is to map data into a high dimensional space and to find the hyper-plane of the different classes with the maximum margin between them. SVMs have been used for image classification (Huang *et al.*, 2002; Zhu *et al.*, 2002; Foody and Mathur, 2004; and Pal and Mather, 2005), soil moisture estimation (Ahmad *et al.*, 2010), image retrieval (Wong and Hsu, 2006), and impervious surface estimation (Esch *et al.*, 2009; Sun *et al.*, in press) for remote sensing studies in recent years. The theory of SVM has been extensively described in the literature (Burges, 1998; and Vapnik 1998). Therefore, only a brief description of the concept of SVM in the framework of classification is given here.

Suppose that training data  $(\mathbf{X}_i, y_i)$  ( $\mathbf{X} \in R^k$ ,  $i=1, \dots, L$ ,  $L$  is the number of the training samples and  $y_i \in \{+1, -1\}$  is the class label of the training vector  $\mathbf{X}_i$ ) can be linearly separated by a hyperplane (Eq. (1)):

$$\mathbf{W} \cdot \mathbf{X} + b = 0 \quad (1)$$

Where, the symbol  $\mathbf{W}$  is a weight vector and  $b$  is a scalar, often referred to as a bias.

To describe the separating hyperplane, let us use the following form:

$$\begin{cases} \mathbf{X}_i \cdot \mathbf{W} + b \geq +1 & \text{for } y_i = +1 \\ \mathbf{X}_i \cdot \mathbf{W} + b \leq -1 & \text{for } y_i = -1 \end{cases} \quad (2)$$

The separating hyperplane that creates the maximum margin is called the Optimal Separating Hyperplane (OSH). The goal of the learning process based on SVM is to find the OSH to separate the training data by solving the following quadratic optimization problem:

$$\text{Minimize } \frac{1}{2} \|\mathbf{w}\|^2 + C \left( \sum_{i=1}^L \xi_i \right)$$

Subject to:

$$\begin{cases} y_i [\mathbf{W} \mathbf{X}_i + b] \geq 1 - \xi_i \\ \xi_i \geq 0, i = 1, 2, \dots, L \end{cases} \quad (3)$$

Where the symbol  $C$  denotes a penalty parameter on the training error;  $\xi_i$  is called the slack variables. The calculations can be simplified by converting the problem with Kuhn-Tucker conditions into equivalent Lagrange dual problem.

$$W(\alpha) = \sum_{i=1}^L \alpha_i - \frac{1}{2} \sum_{i,j=1}^L \alpha_i \alpha_j y_i y_j K(\mathbf{X}_i, \mathbf{X}_j) \quad (4)$$

Subject to:

$$\sum_{i=1}^L \alpha_i y_i = 0, \quad 0 \leq \alpha_i \leq C, \quad i = 1, 2, \dots, L \quad (5)$$

Where  $i = 1, \dots, L$  is the sample size and the final decision function is given by

$$f(\mathbf{X}) = \sum_{i=1}^N \alpha_i y_i K(\mathbf{X}_i, \mathbf{X}_j) + b \quad (6)$$

In Equations (5) and (6),  $\alpha_i$  denotes Lagrange multipliers; the parameter  $N$  (usually  $N \ll L$ ) stands for the number of the selected points or support vectors; and the symbol  $K(\mathbf{X}, \mathbf{X}_i)$  is the kernel function that measures non-linear dependence between the two input variables  $\mathbf{X}$  and  $\mathbf{X}_i$ . Three admissible kernel functions include: polynomial kernel function, radial basis kernel function (RBF), and sigmoid kernel function.

The steps involved in SVM modeling are: (1) selecting a suitable kernel function and kernel parameter (kernel width  $G$ ) and (2) specifying the penalty parameter  $C$ . In our paper, a RBF kernel is used for constructing the classifier. In addition, specifying parameters  $G$  and  $C$  is the key step in SVM because their combined values determine the boundary complexity and thus the classification performance (Devos *et al.*, 2009). In our research, the kernel width  $G$  was set to 0.15 and the penalty parameter was set to 100 (Sun *et al.*, in press). For the implementation of the training and modeling procedure, we employed the existing SVM library LIBSVM presented by Chang and Lin (Chang and Lin, 2008). The LIBSVM represents integrated software for SVM classification, regression, distribution estimation and multi-class classification. In order to keep the classification runtime low, the maximum numbers of training and testing samples for a given class do not exceed 3000 and 5000.

## L-THIA Model Description

The L-THIA model was developed to estimate direct runoff using the curve number (CN) method from daily rainfall depth, LULC, and hydrologic soil group data (Harbor, 1994). It provides a quick and simple impact analysis for initial plan review and for community awareness of potential long-term problems (Harbor *et al.*, 1998). For runoff calculation, L-THIA uses the curve number (CN) method of the US Department of Agriculture (USDA) Soil Conservation Service (SCS, now Natural Resources Conservation Service), which is a core component of many traditional hydrology models (Wang *et al.*, 2005). The runoff equation is:

$$Q = \frac{(P - I_a)^2}{(P - I_a) + S} \quad (7)$$

Where  $Q$  is the runoff (inch),  $P$  is the rainfall (inch),  $S$  is the potential maximum retention after runoff begins (inch), and  $I_a$  is the initial abstraction (inch) and can be approximately estimated by

$$I_a = 0.2S \quad (8)$$

$S$ , in  $mm$ , is related to the soil and LULC conditions and can be described by CN through:

$$S = \frac{25400}{CN} - 254 \quad (9)$$

Where CN is determined by the combination of LULC and soil (hydrological soil group) information for each cell. Theoretically, CN values are between 0 and 100. However, practically, CN values change between 30 and 100. Then, L-THIA model uses daily rainfall series and the CNs to calculate the mean of annual total surface runoff both in terms of depth and volume (Wang *et al.*, 2005).

As illustrated in Equations (7)-(8), L-THIA model requires long-term daily precipitation data, soils GIS, and LULC GIS data. Daily precipitation series for the period of 1978–2009 were obtained from the meteorological department. Soils GIS data are required as a hydrological soil group (HSG). The soil GIS data was obtained from the Soil and Fertilizer Workstations of Beijing. The LULC GIS data was derived from Landsat TM/ETM+ imagery (acquired in 1986, 1992, 1999, 2006, and 2009 respectively) using support vector machine (SVM) method.

## RESULTS AND ANALYSIS

### LULC Change

In our research, we grouped the LULC types into seven categories: (1) high impervious surface (> 90%, high-density urban, including CBD, roads, squares and so on), (2) medium impervious surface (50% ~ 90%, high-density residential land), (3) low impervious surface (< 50%, low-density residential land), (4) arable land (agricultural land), (5) forest land, (6) bare land, and (7) water body. Fig. 4 and 5 illustrate the percentages and spatial distributions of LULC classes in the Beijing region from 1986 to 2009. Forest and arable lands dominated in the whole area but decreased with the continuous increase of urban areas, especially agricultural land. The urbanization level (high impervious surface), the proportion of urbanized area to the total land area, was 4.18%, 4.28%, 6.03%, 8.34%, and 12.78% in 1986, 1992, 1999, 2006, and 2009, respectively. The proportion of residential area to the total land area was 3.09%, 3.21%, 3.15%, 3.83%, and 6.66% in 1986, 1992, 1999, 2006, and 2009, respectively. Urban areas increased from 4.18% in 1986 to 12.78% in 2009, and residential areas increased from 3.09% in 1986 to 6.66% in 2009; while agricultural land areas decreased from 24.69% in 1986 to 11.44% in 2009.

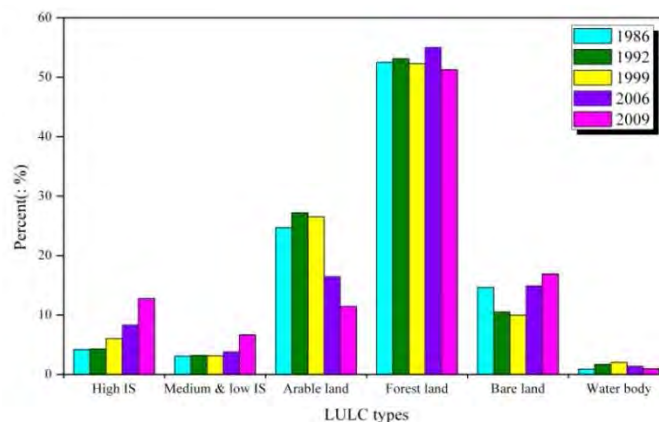


**Figure 4.** Variations of percentages of LULC types in whole study area.

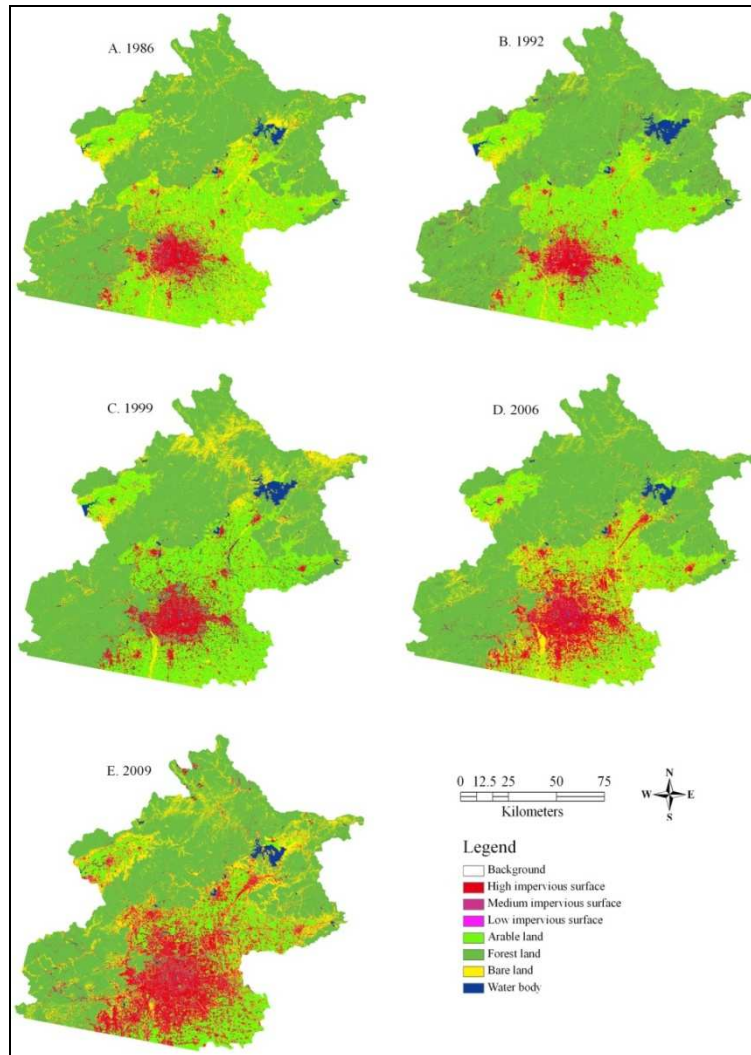


**Figure 5.** The LULC maps of the Beijing region in 1986, 1992, 1999, 2006, and 2009.

From Fig. 5, we can observe that Beijing’s development pattern is a typical concentric expansion; showing a ring-shaped pattern. In the LULC maps of 1986 and 1992 (Fig. 5A and 5B), Forest and arable lands dominated in the whole area, and there was little change in urban areas. The LULC map in 1999 (Fig. 5C) indicated that urban areas started to expand to around the city. In the LULC map of 2006 (Fig. 5D), urban areas dominated in the Beijing region. Large areas, especially arable lands, were converted to urban areas. In the LULC map of 2009 (Fig. 5E), urban areas continuously increased, becoming the dominant LULC type and continuously extending into around the city.

In summary, the selected areas experienced rapid LULC change, especially urbanization, from 1986 to 2009. Spatially, Beijing’s urbanization pattern is a typical concentric expansion. Temporally, the urbanization rate was relatively low in the end of 1980s and accelerated after 1999.

### **Determination of Model Parameters**

According to the L-THIA model, CN value is determined by the combination of LULC types and soil

(hydrological soil group) information for each cell. The LULC types were derived from Landsat TM/ETM+ imagery as described earlier. According to soil classification categories in L-THIA model, the soil data obtained from the Soil and Fertilizer Workstations of Beijing was reclassified to output the soil hydrological map using ARCVIEW software. Based on CN values in the L-THIA model, local soil infiltration properties and other published results, CN values in the Beijing region were estimated and showed in Table 1.

**Table 1. Estimated CN values**

LULC types	Land surface infiltration categories			
	A	B	C	D
Water body	0	0	0	0
High-density urban	90	93	94	95
Arable land	67	78	85	89
high-density residential	77	85	90	92
low-density residential	61	75	83	87
Bare land	72	82	88	90
Forest land	30	55	70	77

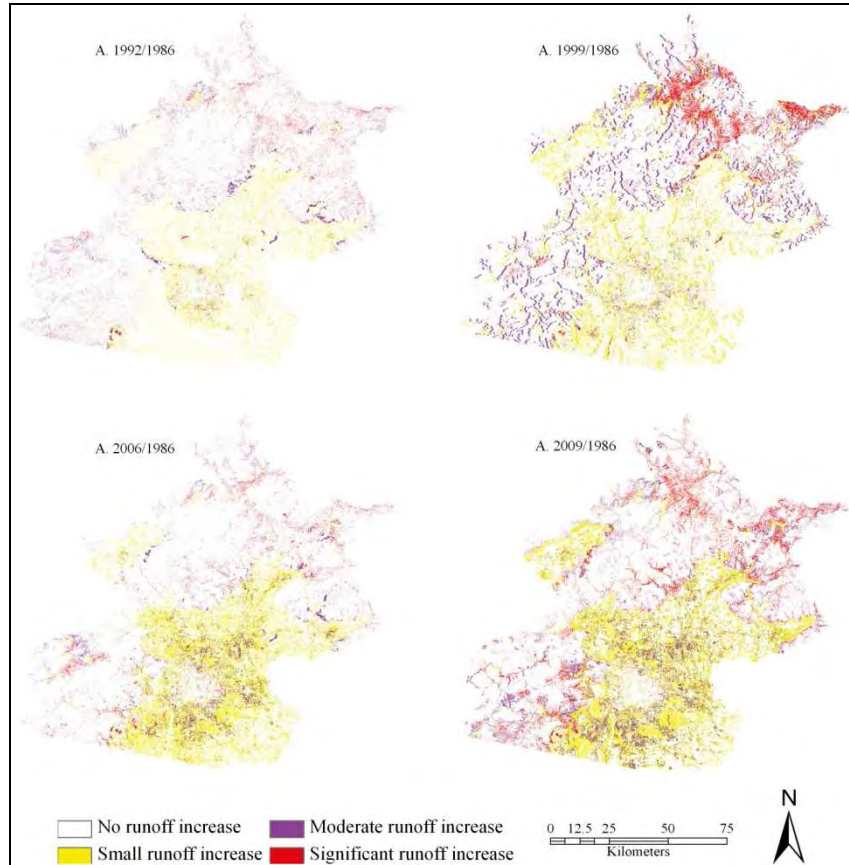
Land surface infiltration categories: A: high infiltration rate; B: moderate infiltration rate; C: low infiltration rate; D: very low infiltration rate.

### Modeled Runoff Variations

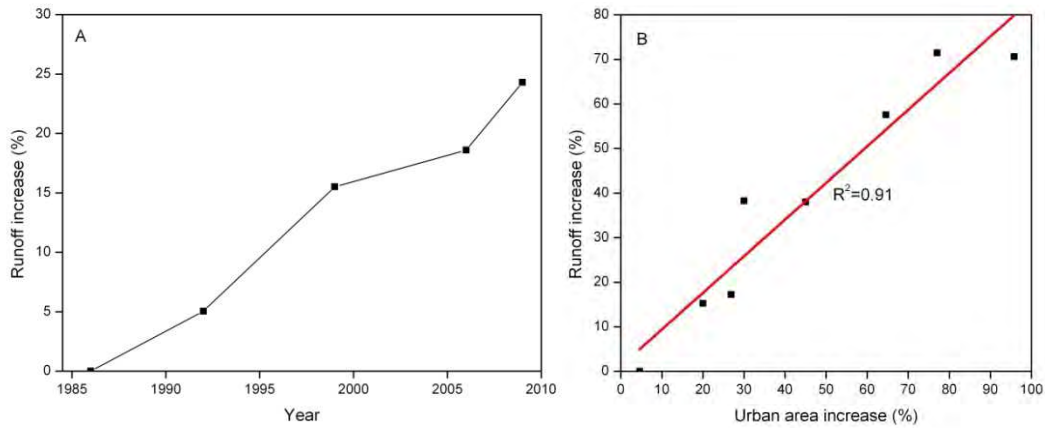
In our research, the L-THIA model was used to simulated annual average runoff for 1986, 1992, 1999, 2006, and 2009. The long-term impacts of LULC change on surface runoff were then assessed. The simulated runoff for 1986 as the reference, a runoff change ratio for a certain year (such as 1992) can be calculated using the runoff simulated for that year divided by the runoff simulated for 1986. This runoff change ratio can be used to assess the spatial distribution of runoff variations due to the LULC change (Li and Wang, 2009). Then, the ratios were divided into four categories: (1) no runoff increase (ratio  $\leq 1.0$ ); (2) small runoff increase ( $1.0 < \text{ratio} \leq 2.0$ ); (3) moderate runoff increase ( $2.0 < \text{ratio} \leq 3.5$ ); and (4) significant runoff increase (ratio  $> 3.5$ ).

Fig. 6 showed spatial distribution of modeled runoff change in 1992, 1999, 2006, and 2009 compared to the reference in 1986. Compared to the modeled runoff for 1986, spatial variation of runoff change in 1992 was limited (Fig. 6A). A moderate and significant runoff increase became apparent in 1999 (Fig. 6B) and continued in 2006 (Fig. 6C). In 2003, areas of moderate and significant runoff increase dominated in the whole study area (Fig. 6D).

Fig. 7A showed runoff increase percentage of 1992, 1999, 2006, and 2009 compared to 1986. From the Fig. 7A, we observed that a runoff increase 25% from 1986 to 2009 for the whole area. The runoff increase was relatively low from 1986 to 1992 and much higher in the 1999. In 2006 and 2009, the runoff increase continued. Fig. 7B showed the relationship between runoff increase and the percentage of urban areas increase. Strong and positive relationships ( $R^2 = 0.91$ ) were observed between the runoff increase and the percentage of urban areas increase in the whole watershed (Fig. 7B). Our results indicated that the runoff increase was highly correlated with urban expansion.



**Figure 6.** Spatial distribution of modeled runoff change in 1992, 1999, 2006, and 2009 compared to the reference in 1986.



**Figure 7.** A. Runoff increase percentage of 1992, 1999, 2006, and 2009 compared to 1986. B. Relationship between runoff increase and the percentage of urban areas increase.

## CONCLUSIONS

This paper presented a case study to investigate the long-term impacts of LULC change on surface runoff in fast urbanizing Beijing city, the capital of China. The LULC maps were derived from Landsat TM/ETM+ imagery (acquired in 1986, 1992, 1999, 2006, and 2009 respectively) using support vector machine (SVM) method. A simpler-to-use L-THIA model was applied to simulate surface runoff variations in the study area from 1986 to 2009. The long-term impacts of urbanization on surface runoff were then assessed.

Results indicated that the selected study area experienced rapid urbanization from 1986 to 2009. In the whole area, urban areas increased from 4.18% in 1986 to 12.78% in 2009, and residential areas increased from 3.09% in 1986 to 6.66% in 2009; while agricultural land areas decreased from 24.69% in 1986 to 11.44% in 2009. As a direct result of the urbanization from 1986 to 2009, the long-term surface runoff increased 25% for the whole area. Our results also indicated that the runoff increase was highly correlated with the percentage of urban areas increase ( $R^2 = 0.91$ ). This research can provide a simple method for policy makers to assess potential hydrological impacts of future planning and development activities.

## ACKNOWLEDGEMENTS

This research in this paper was sponsored by the National Basic Research Program of China (also called 973 Program, No. 2009CB723906) for a project entitled “Earth Observation for Sensitive Factors of Global Change: Mechanisms and Methodologies”, and graduate technological innovation program of Chinese Academy of Sciences. The authors would like to thank the Soil and Fertilizer Workstations of Beijing for providing the soil type classification map. The authors would also like to thank Prof Yingkui Li (Department of Geography, University of Tennessee) for helpful discussion on improving the presentation of this paper.

## REFERENCES

- Agriculture (USDA), Soil Conservation Service, 1986. Urban hydrology for small watersheds, Washington, DC: USDA Natural Resources Conservation Service, Engineering Division, Technical Release 55.
- Ahmad, S., A. Kalra and H. Stephen, 2010. Estimating soil moisture using remote sensing data: A machine learning approach, *Advances in Water Resources*, 33(1): 69–80.
- Arnold, J. G., R. Srinivasan, R. S. Muttiah, and J. R. Williams, 1998. Large-area hydrologic modeling and assessment: Part I. Model development, *Journal of American Water Resources Association*, 34: 73–89.
- Brun, S.E., and L.E. Band, 2000. Simulating runoff behavior in an urbanizing watershed, *Computers, Environment and Urban Systems*, 24: 5-22.
- Burges, C. J. C., 1998. A tutorial on support vector machines for pattern recognition, *Data Mining and Knowledge Discovery*, 2(2):121-167.
- Chang, C. C., and C. J. Lin, 2008. LIBSVM: *A Library for Support Vector Machines*. Department of Computer Science and Information Engineering, National Taiwan University, Taiwan. Available online at: <http://www.csie.ntu.edu.tw/~cjlin/libsvm> (accessed 15 October 2008).

- Devos, O., C. Ruckebusch, A. Durand, L. Duponchel and J.-P. Huvenne, 2009. Support vector machines (SVM) in near infrared (NIR) spectroscopy: Focus on parameters optimization and model interpretation, *Chemometrics and Intelligent Laboratory Systems*, 96(1): 27-33.
- Esch, T., V. Himmler, G. Schorcht, M. Thiel, T. Wehrmann, F. Bachofer, C. Conrad, M. Schmidt and S. Dech, 2009. Large-area assessment of impervious surface based on integrated analysis of single-date Landsat-7 images and geospatial vector data, *Remote Sensing of Environment*, 113(8):1678–1690.
- Foody, G. M., and A. Mathur, 2004. A relative evaluation of multiclass image classification by support vector machines, *IEEE Transactions on Geoscience and Remote Sensing*, 42(6): 1335-1343.
- Harbor, J. M., M. Grove, B. Bhaduri, and M. Minner, 1998. Long-term hydrologic impact assessment (L-THIA) GIS, *Public Works*, 129:52–54.
- Harbor, J., 1994. A practical method for estimating the impact of land use change on surface runoff, groundwater recharge and wetland hydrology, *Journal of American Planning Association*, 60: 91–104.
- Huang, C., L. S. Davis, and J. R. G. Townshend, 2002. An assessment of support vector machines for land cover classification, *International Journal of Remote Sensing*, 23(4): 725-749.
- Huber, W., R. Dickenson, L. Roesner, and J. Aldrich, 1988. Storm water management model user's manual, Version 4. Athens, GA: U.S. Environmental Protection Agency.
- Li, Y., and C. Wang, 2009. Impacts of urbanization on surface runoff of the Dardenne Creek watershed, St. Charles County, Missouri, *Physical Geography*, 30(6): 556–573.
- Lim, K.J., B.A. Engel, Z. Tang, S. Muthukrishnan, J. Choi, and K. Kim, 2006. Effects of calibration on L-THIA GIS runoff and pollutant estimation, *Journal of Environmental Management*, 78: 35-43.
- Lin, Y.-P., N. M. Hong, P. J. Wu, and C. J. Lin, 2007. Modeling responses of hydrologic processes to future watershed land use scenarios and climate change in an urbanized watershed in Taiwan, *Environmental Geology*, 53:623–634.
- Ng, H. Y. F., and J. Marsalek, 1989. Simulation of the effects of urbanization on basin stream flow, *Water Resources Bulletin*, 25: 117-124.
- Pal, M., and P. M. Mather, 2005. Support vector machines for classification in remote sensing, *International Journal of Remote Sensing*, 26(5):1007-1011.
- Shi, P., Y. Yuan, J. Zheng, J. Wang, Y. Ge, and G. Qiu, 2007. The effect of land use/cover change on surface runoff in Shenzhen region, China, *Catena*, 69: 31-35.
- Sun, Z., H. Guo, X. Li, L. Lu, and X. Du, (in press). Estimating urban impervious surfaces from Landsat-5 TM imagery using multi-layer perceptron neural network and support vector machine, *Journal Applied of Remote Sensing*.
- Vapnik, V. N., 1995. *The Nature of Statistical Learning Theory*, Springer-Verlag, New York.
- Vapnik, V. N., 1998. *Statistical Learning Theory*, Wiley, New York.
- Wang, Y., C. Woonup, and M. D. Brian, 2005. Long-term impacts of land-use change on non-point source pollutant loads for the St. Louis metropolitan area, USA, *Environmental Management*, 35(2): 194-205.
- Weng, Q., 2001. Modeling urban growth effects on surface runoff with the integration of remote sensing and GIS, *Environmental Management*, 28(6): 737-748.
- Wong, W. -H., and S. -H. Hsu, 2006. Application of SVM and ANN for image retrieval, *European Journal of Operational Research*, 173(3):938–950.
- Yang, L., G. Xian, J. M. Klaver and B. Deal, 2003. Urban land-cover change detection through sub-pixel

imperviousness mapping using remotely sensed data, *Photogrammetric Engineering and Remote Sensing*, 69(9): 1003-1010.

Zheng, J., W. Fang, P. Shi, and L. Zhuo, 2009. Modeling the impacts of land use change on hydrological Processes in fast urbanizing region —A case study of the Buji watershed in Shenzhen City, China, *Journal of Natural Resources*, 24(9): 1560–1572.

Zhu, G., and D. G. Blumberg, 2002. Classification using ASTER data and SVM algorithms: The case study of Beer Sheva, Israel, *Remote Sensing of Environment*, 80 (2): 233-240.